Shear and punching capacity predictions for slabs under concentrated loads aided by lefea

de Sousa, Alex M.D.; Lantsoght, Eva O.L.; Setiawan, Andri; El Debs, Mounir K.

SHEAR AND PUNCHING CAPACITY PREDICTIONS FOR SLABS UNDER CONCENTRATED LOADS AIDED BY LEFEA

Alex M. D. de Sousa, Eva O. L. Lantsoght, Andri Setiawan and Mounir K. El Debs

Synopsis: One-way slabs under concentrated loads may fail by one-way shear, punching, flexure or a mixed-mode between them. This study examines the benefits of using Linear Elastic Finite Element Analyses (LEFEA) combined with analytical expressions to predict the shear and punching capacities of such slabs. Besides, the determination of the most critical shear failure mechanism is also addressed. A simplified approach is proposed to predict the shear and punching capacity without numerical models. Forty-eight tests of simply supported slabs under concentrated loads were evaluated. The LEFEA was conducted with ABAQUS. The analytical expressions are based on the Critical Shear Crack Theory (CSCT). The coupling of the CSCT-expressions with the LEFEA accurately predicts the governing shear failure mechanism and the shear capacity of most test results. In this study, it was also found that the punching capacity predictions may be improved by considering the influence of the slab width and load size on the governing failure mechanism. A similar level of precision was achieved using only analytical expressions when properly calibrated. Therefore, the CSCT expressions can be used at different stages of design and assessment of existing structures according to the Level of Approximation required.

ACI student member **Alex M. D. de Sousa** is a Ph.D. Candidate at the São Carlos School of Engineering (EESC) from the University of São Paulo (USP), São Carlos, Brazil. His research interests include the shear, punching shear and numerical modeling of reinforced concrete structures.

ACI member **Eva O. L. Lantsoght** is a Full Professor at Universidad San Francisco de Quito, and an Assistant Professor at the Delft University of Technology. She is the Vice-Chair of ACI 445-0E Torsion, member of ACI 445-0D Shear Databases, ACI 342, Evaluation of Concrete Bridges and Bridge Elements, and ACI-ASCE 445, Shear and Torsion, Secretary of ACI-ASCE 421, Design of Reinforced Concrete Slabs, and an associate member of ACI 437, Strength Evaluation of Existing Concrete Structures.

ACI member **Andri Setiawan** is a former Postdoctoral Researcher at École Polytechnique Fédérale de Lausanne (EPFL), Switzerland. He received his Ph.D. in structural engineering from Imperial College London, UK, in 2019. He is a representative of *fib* (The International Federation for Structural Concrete) in the ACI 318-L committee. His research interest includes shear, punching shear, seismic design of concrete structures and dissipative systems, and numerical modeling.

ACI member **Mounir K. El Debs** is a Senior Professor at the São Carlos School of Engineering (EESC) from the University of São Paulo (USP), São Carlos, Brazil. He received his MSc and Ph.D. in structural engineering from EESC-USP in 1976 and 1984, respectively. His research interests include reinforced and prestressed concrete, precast concrete, and thin-walled concrete elements.

INTRODUCTION

One-way slabs under large concentrated loads are commonly found in practice in bridge deck slabs but may also occur during the building or use of residential and industrial floor slabs. Typically, the one-way shear capacity for such members is checked by assuming that only a slab strip of a width called the effective shear width, contributes to the sectional shear capacity[1] (Figure 1a). In this approach, the shear forces are assumed as uniformly distributed on the effective shear width. Conversely, the punching capacity predictions are usually performed with the same expressions derived from slab-to-column connections under concentric loads and assuming a uniform distribution of punching shear stresses around the shear-resisting control perimeter[2] (Figure 1b). In reality, the shear forces are not evenly distributed on the critical sections for one-way shear and punching shear and depend on parameters such as the load position[3] and slab width[4]. Consequently, if the assumed distribution of shear stresses on the critical sections for shear and punching deviates a lot from the assumed ones in the analytical expressions, inconsistent shear and punching capacity predictions may be found.
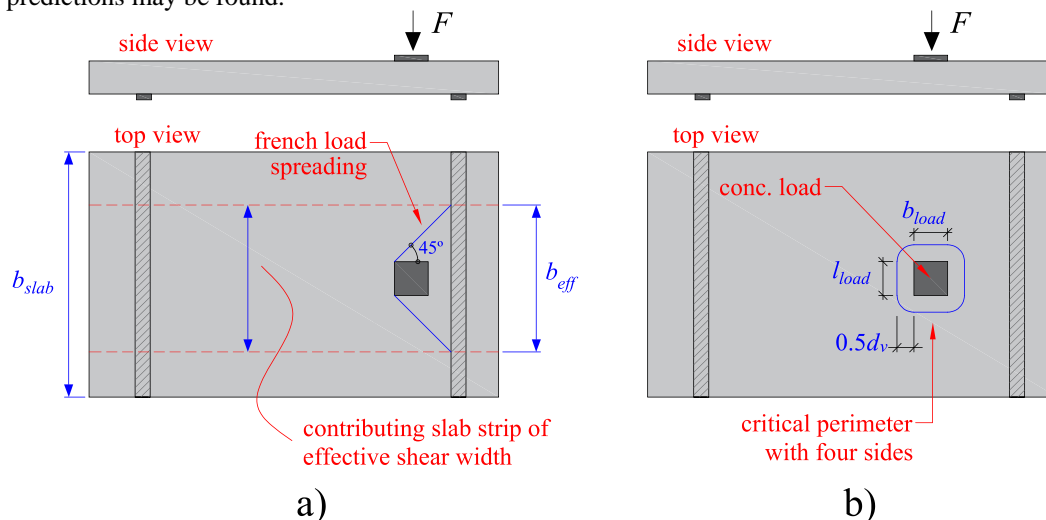

Figure 1 - General approaches to evaluate the a) one-way shear and b) punching capacity of one-way slabs under concentrated loads.

When evaluating the one-way shear capacity of slabs under concentrated loads, the effective shear width used has a marked influence on the predictions[2,5]. A common approach to predict the effective shear width at failure is based on

a horizontal spreading of the load under a 45º angle from the back sides of the load, also called the French effective shear width as it is used in the French guidelines[6,7] (Figure 1a). However, a number of studies have already pointed out some shortcomings related to this approach, which should be considered in the assessment of existing structures[5,8]. While this approach provides good accuracy to predict the sectional shear capacity of slabs under concentrated loads close to the support ($a_v < 2d_l$)[1,2,9], unconservative results may be found for loads further away from the support[5,8]. For instance, the predicted sectional shear capacity may overestimate the sectional shear significantly at failure[2,5], mainly when the tests fail by punching instead of one-way shear. As a consequence, changes are required in the predicted effective shear width to assure conservative predictions of sectional shear capacity for tests that may be at the transition point to punching shear failure modes, a topic which is seldomly discussed in the literature.

In turn, the punching capacity of one-way slabs under concentrated loads is considerably less discussed than the one-way shear capacity. Until now, most evaluations of the punching capacity of one-way slabs were performed using only semi-empirical code expressions[2,10]. These investigations found a large scatter between theoretical and tested resistances, mainly when the tests fail by one-way shear or a transitional shear failure mode instead of punching[2].

In 2015, Natário[11] presented an interesting approach to assess the shear and punching capacity of one-way slabs under concentrated load. This approach was based on using the Critical Shear Crack Theory (CSCT) expressions for shear and punching and estimating parameters such as the shear force and bending moment distribution based on Linear Elastic Finite Element Analysis (LEFEA). Figure 2 shows the results of predictions by Natário[11] for 48 simply supported slabs using the proposed approach for one-way shear (Figure 2a) and for two-way shear (Figure 2b) as a function of the clear shear span to effective depth ratio (a_v/d_l). a_v is the clear shear span: distance between edge of support and edge of load. In Figure 2, all result values were taken directly from the tables of Natário's dissertation[11] and presented herein in figure format. V_{test} and $V_{predicted}$ are the maximum sectional shear achieved in the tests and the predicted shear resistance by Natário[11], respectively; P_{test} and $P_{predicted}$ are the maximum applied concentrated load at failure and the punching capacity predicted by Natário[11], respectively. In the proposed approach by Natário[11], the effective shear width b_{eff} for one-way shear and the control perimeter for two-way shear calculations account for the uneven distribution of shear forces in the evaluated sections and regions. The effective shear width, for instance, was calculated by the relation between the total shear force $V_{control}$ (force unit) and an averaged shear force v_{avg} (unit of force per unit length) determined on a specific control section of the slab. Consequently, this approach allows considering the spatial load transfer towards the support and distribution of inner forces in the slab in a more realistic way. These parameters were calculated aided by LEFEA, such as will be described in more detail in the next sections. Figure 2a shows that the predictions of one-way shear capacity with the presented approach were precise and conservative (on average) regardless of the failure mode of the tests being wide beam shear (WB), punching (P) or a mixed-mode between wide beam shear and punching shear (WB+P). However, the presented approach presented a small shortcoming in the punching predictions (Figure 2b). Figure 2b shows that the predictions of punching capacity for the tests that failed as wide beams in shear (WB) are on the unsafe side. At this point, this does not represent a serious problem since, in practice, the one-way shear predictions are governing (more conservative) in the calculations. In other words, the proposed approach by Natário[11] captures that the concentrated load to cause a wide beam shear failure is lower than that to cause a punching failure since $V_{test}/V_{predicted}$ is higher than $P_{test}/P_{predicted}$ for such tests. Figure 2c shows, for instance, that combining the predictions of one-way shear and punching to identify the most critical strength ratio (SR = max$\{V_{test}/V_{predicted}; P_{test}/P_{predicted}\}$), the proposed approach by Natário[11] provides safe and precise predictions of the shear capacity. However, it is clear that improvements may be included in the proposed approach for punching calculations to reach a similar performance as for the one-way shear predictions.

For a preliminary assessment of slabs, the use of LEFEA is frequently not common. In practice, simplified and conservative calculation models are applied in preliminary evaluations, and LEFEA is used when more precise estimations are required. According to the design philosophy included in the current *fib* Model Code 2010[12], detailed methods could be simplified in a conservative way to allow reaching quick and conservative predictions of resistance. This approach of using simplified and detailed expressions keeping the same theoretical background is also called the "Levels of Approximations Approach," and it was implemented in the shear and punching expressions of the *fib* Model Code 2010[12]. In this way, someone could question how to perform simplified estimations of shear and punching capacity for the tests evaluated by Natário[11] with the CSCT expressions without the use of numerical models, which was not addressed by Natário[11]. In the literature, it was identified that simplified approaches to evaluate the shear capacity of one-way slabs under concentrated loads without accounting for both possible shear failure modes might lead to unsafe predictions of resistance[2,5,10]. Moreover, most studies focus on evaluating cantilever slabs[3,5,13,14].

Therefore, further investigations are required to provide guidelines to assess both shear and punching capacities of simply supported slabs under concentrated loads using only analytical expressions.
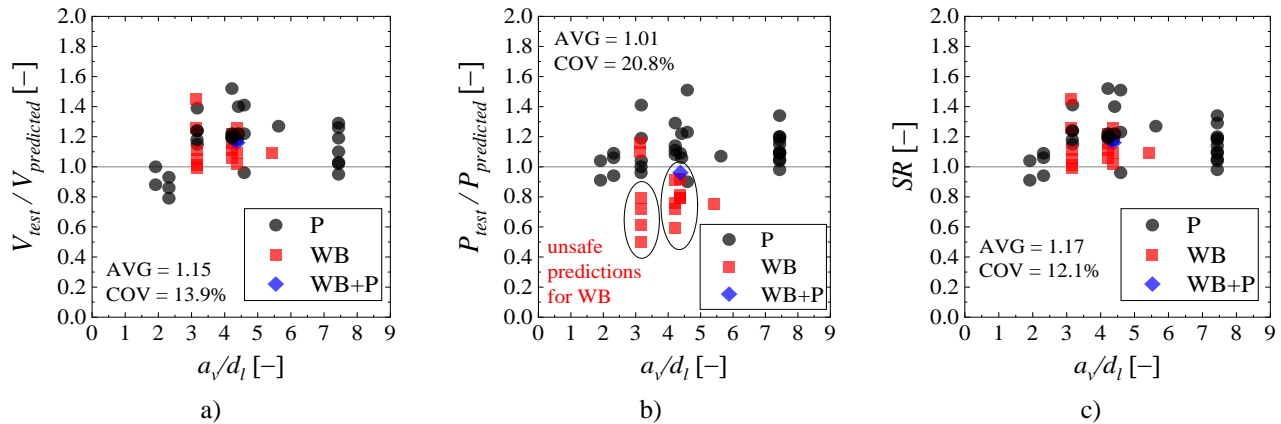

Figure 2 - Relation between tested and predicted resistances for a) one-way shear; b) punching shear and c) considering the most critical relation (conservative prediction) between the one-way shear and punching shear predictions reported by Natário[11].

In this study, a fully analytical approach is proposed to evaluate the shear and punching capacity of one-way slabs under concentrated loads based on the CSCT expressions. Parameters such as the load position, slab width and load size were considered in the proposed approach. First, an approach of a higher Level of Approximation (LoA) to predict the shear and punching capacities of such slabs inspired by the work of Natário[11] is described using LEFEA. This approach uses LEFEA to estimate parameters of the CSCT expressions, such as the bending moment and unitary shear force on the critical sections. In this study, the punching capacity approach of Natário[11] was enhanced by including parameters related to the slab width and load size. In a next step, it is described how parameters and expressions from the refined approach using LEFEA can be estimated or considered in a simplified approach to predict the shear and punching capacity of the slabs also using the CSCT expressions. In the end, both approaches are compared.

RESEARCH SIGNIFICANCE
Nowadays, the use of Linear Elastic Finite Element Analyses (LEFEA) in the design of new structures and assessment of existing structures has become common practice. However, a limited number of studies provide detailed guidelines on how to use this tool together with one-way shear and punching shear expressions. Therefore, this paper provides detailed guidance on how to use LEFEA to predict the shear and punching capacity of one-way slabs under concentrated loads. In addition, a simplified approach using only analytical expressions is proposed for the preliminary design or assessment of existing structures. Both approaches are based on the Critical Shear Crack Theory expressions, which is based on the mechanics of the shear problem.

BACKGROUND
Shear flow
The shear flow of one-way slabs under concentrated loads combines characteristics from the one-way shear in beams and the two-way shear around slab-to-column connections[3,15]. Beams and slabs loaded over the entire width develop a shear flow predominantly unidirectional, with the flow lines parallel to each other along the slab width. Flat slabs under concentric loads create a shear flow with lines radially distributed around the load. In Figure 3a, for the case of one-way slabs under concentrated loads, the shear flow lines are almost parallel in the vicinity of the support, such as for beam shear, while its distributions assume a radial pattern around the load typical from punching[3]. Considering the shear flow characteristics, both shear failure modes may take place for such slabs.

Analytical approaches to evaluate the shear and punching capacity
Current approaches to predict the one-way shear capacity of slabs subjected to large concentrated loads are based on the assumption of a horizontal load spreading with a 45° angle to the support for defining the contributing width, commonly called the effective shear width (see Figure 3b). Over this length, the unitary shear stresses are assumed as constant. This approach is well spread in the literature since it provided fair approximations of the maximum bending moments at the support of cantilever slabs[16]. However, several works demonstrated that the maximum unitary shear

forces at the support could be underestimated with these approaches[11,16,17]. Because of this, LEFEA became an interesting tool to estimate a more realistic distribution of shear stresses and bending moments on slabs. The punching capacity calculations using analytical methods are also based on the assumption of even distribution of shear stresses on the control perimeter for punching regardless of the load position in the span (Figure 3c.1), where statics lead to nonproportional shear loading on the front and back faces of the loading plate unless the load is placed at midspan. The use of LEFEA allows considering the uneven distribution of shear stresses around the control perimeter (Figure 3c.2) and, in this way, determining a reduced (effective) control perimeter accounting for the load layout and boundary conditions[18].
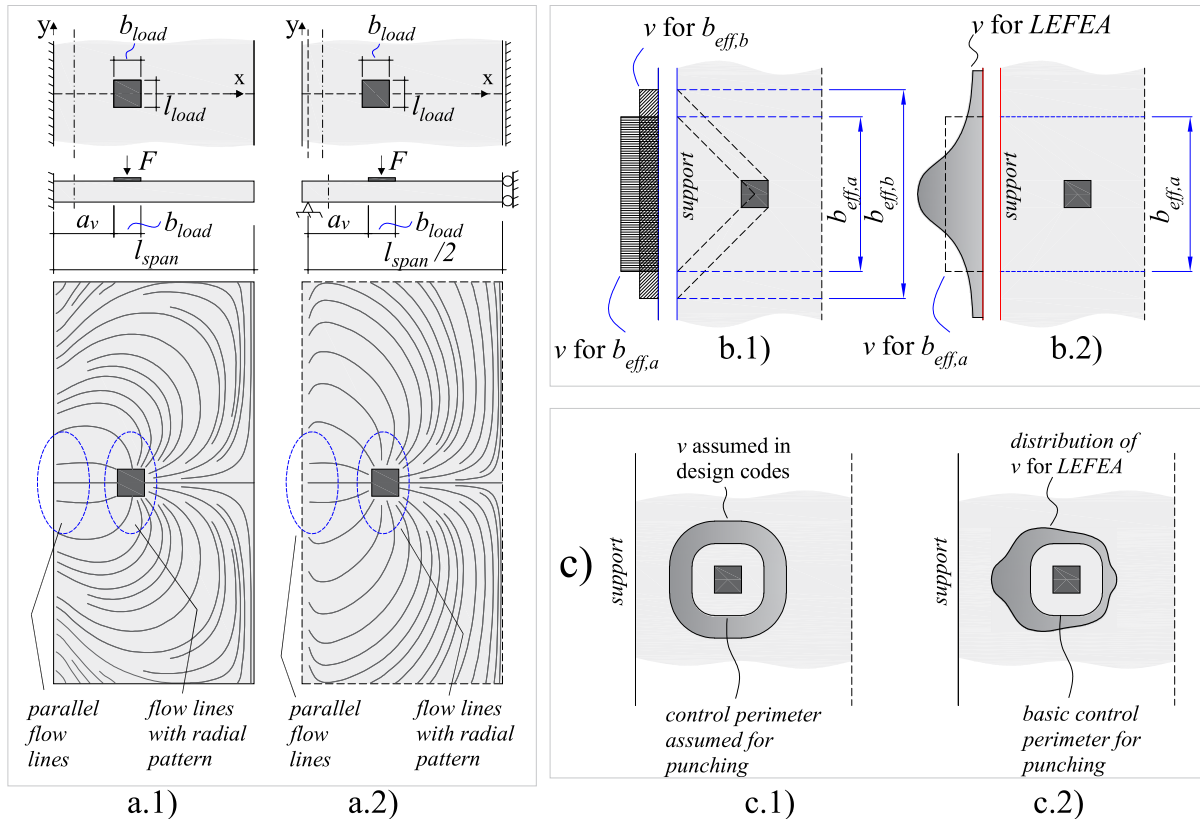

Figure 3 - Shear flow in a.1) cantilever slabs and a.2) simply supported slabs under symmetrical concentrated loads (adapted from Natário et al. [3]); b) assumed distribution of shear stresses at the support by analytical models of effective shear width (b.1) and captured by LEFEA (b.2), and c) distribution of shear stresses on the control perimeter for punching assumed in simplified calculations (c.1) and captured by LEFEA (c.2).

Effective shear width and reduced control perimeter based on LEFEA

Two groups of approaches can be distinguished when using the LEFEA to evaluate the one-way shear capacity of slabs under concentrated loads: (i) one is based on the definition of an effective shear width as proposed by Goldbeck[19] to be multiplied by the unitary shear strength; the comparison between load effects and sectional resistances is made in terms of force[3]; (ii) others are based on the definition of a distribution width on which the peak shear stress from LEFEA are averaged (rounded/distributed) to be compared to the code-based unitary shear strength[20]; the comparison between load effect and resistances is made in terms of unitary forces or shear stresses.

The effective width is determined based on the stress or force distribution over the member's width v_{perp}[19,21]. The classical definition is that the resisting action due to the maximum shear force $v_{perp,max}$ distributed over the effective width b_{eff} equals the resisting action due to the variable stresses over the entire width[22] (see Figure 4a). Here, $v_{perp,max}$ is the maximum value of the unitary or nominal shear force (i.e., shear force per unit length along the control section). Some studies proposed distributing the peak shear force over a certain length (calculating v_{avg}) and calculating the effective shear width based on the averaged shear force v_{avg} instead of peak values $v_{perp,max}$. This approach aims to consider possible redistribution of shear force due to concrete cracking[3,23]. As b_{eff} increases by decreasing v, the predicted effective shear widths increase with these modified approaches.
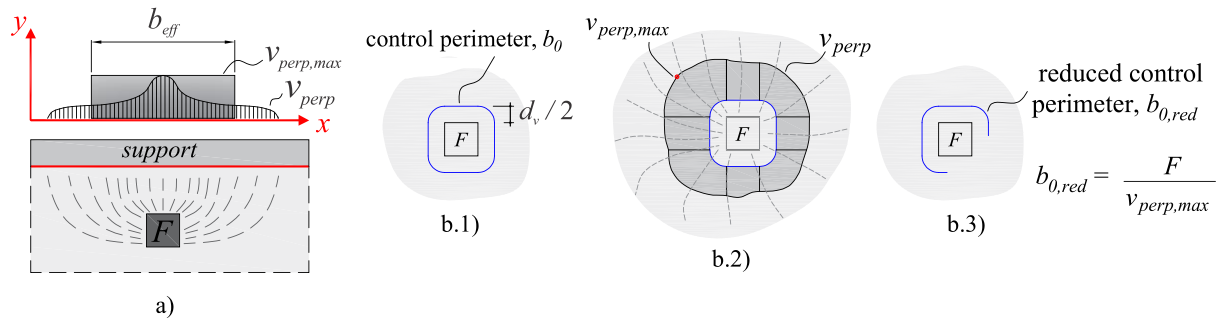
Figure 4 – (a) Definition of the effective shear width based on Goldbeck's studies[19]; (b) definition of an effective (reduced) control perimeter based on the uneven distribution of shear stresses around the load (adapted from Fernandez Ruiz et al.[16]).

Lantsoght et al.[20,24] investigated over which distribution width (slab strip) the peak shear stress from LEFEA should be averaged to represent the test results. In other words, it was investigated over which length the peak shear stress should be averaged to provide the shear stress that could be compared to the code-based shear capacity [20]. In their analyses, the loads corresponding to a certain degree of that reached in the tests (40% and 90%) were applied in the numerical models, and the shear stress distribution was evaluated at the supports. Tests instrumented with load cells at the support were used to assess the distribution of experimental reaction forces. The reaction forces were converted into shear stresses assuming that the reaction force was uniformly distributed over the influence length of each bearing point. It was concluded that the peak shear stress from LEFEA could be distributed over a length of $4d_l$ to provide precise and still safe predictions of shear capacity for the test results. Posteriorly, Natário[11] suggested using $4d_l$ as the distribution length to calculate the effective shear width for cantilever slabs and $4d_l + l_{load}$ for simply supported slabs.

For punching, Vaz Rodrigues et al.[18] suggested using a similar approach, based on the effective shear width; to define an effective control perimeter, commonly named reduced control perimeter $b_{0,red}$ (see Figure 4b) rounded corners were assumed as suggested by Muttoni[25] in the CSCT expressions. In practice, using the reduced control perimeter based only on the peak shear demand does not allow considering shear redistribution at failure. This limitation is contoured by evaluating each portion of the control perimeter separately and considering the unequal distribution of shear resistance around the load[26]. This method is referred to as CSCT$(\psi_x - \psi_y)$[26].

While the LEFEA allows a better insight into the distribution of internal forces on the slab (action side), the shear and punching resistances can be predicted based on the CSCT expressions. The CSCT for beam shear and punching shear have some similarities[27]. For shear and punching mechanisms, it is assumed that that the unitary shear strength of members without transverse reinforcement is related to the width w and roughness of the critical shear crack, which develops through the inclined compression strut carrying shear[25,28]. For one-way shear, the opening of the critical shear crack is related to the strains at the control section ε and, hence, of the sectional bending moments m[28]. For punching, the opening of the critical shear crack w is related to the slab rotation ψ around the load, which is also dependent on the internal moments m around the load[25]. In the following sections, more details are given regarding the calculations using the CSCT expressions for shear and punching.

PROPOSED REFINED APPROACH: COUPLING LEFEA AND CSCT EXPRESSIONS

Refined approach for one-way shear analyses
The one-way shear capacity of the slabs was calculated according to the Critical Shear Crack Theory developed by Muttoni and Schwartz[29] and modified by Muttoni and Fernandez Ruiz[28]. The principle of this theory is that the flexural shear strength is governed by a flexural crack which develops diagonally (the critical shear crack) and disturbs the shear transfer actions. The main shear transfer mechanisms of slender beams according to the CSCT are[28]: (i) compression chord capacity or cantilever action[30], (ii) aggregate interlock[31] and (iii) dowel action[32,33]. According to this model, the one-way shear capacity $V_{R,CSCT}$ depends on the sectional geometry, the concrete compressive strength, the critical shear crack width w_{cr} and the crack's roughness. The roughness is assumed as related to the aggregate size d_g[34], while the crack width w_{cr} is supposed to be proportional to the reference longitudinal strain ε times the effective depth of the member d_l. The reference longitudinal strain ε is evaluated in the control section at a depth of $0.6d_l$ from the compression face, assuming that plane sections remain plane and neglecting the tensile strength of the concrete

(which is assumed to behave linear elastically in compression). In the absence of external normal forces, the reference strain ε at the control depth and height of the compression zone c_{flex} are given by[28] (SI units; d_l in m; m_{max} in kN/m; 1 m = 3.3 ft; 1 kN/m = 0.068 kip/ft):

$$c_{flex} = d_l \cdot \rho_l \cdot \frac{E_s}{E_c} \cdot \left(\sqrt{1 + \frac{2 \cdot E_c}{\rho_l \cdot E_s}} - 1 \right) \tag{1}$$

$$\varepsilon = \frac{m_{max}}{b_w \cdot d_l \cdot \rho_l \cdot E_s \cdot \left(d_l - c_{flex}/3 \right)} \cdot \frac{0.6 \cdot d_l - c_{flex}}{d_l - c_{flex}} \tag{2}$$

where m_{max} is the maximum bending moment at the control section for a given applied load, ρ_l is the flexural reinforcement ratio, E_c is the elastic modulus of concrete, E_s is the elastic modulus of steel and c_{flex} is the height of the compression zone in the cross-section. In this way, the unitary shear capacity $v_{R,shear}$ or failure criterion is calculated as (SI units: f_c in MPa; d_g in mm; 1 MPa = 145 psi; 1 mm = 0.04 in.):

$$v_{R,shear} = \frac{d_l \cdot \sqrt{f_c}}{3} \cdot \frac{1}{1 + 120 \cdot \dfrac{\varepsilon \cdot d_l}{16 + d_g}} \tag{3}$$

where d_g is the measured maximum aggregate size [0.64 in.] if $f_c < 70$ MPa [10,150 psi] and 0 if higher. The one-way shear capacity is calculated by combining the predicted unitary shear strength $v_{R,shear}$ with an effective shear width b_{eff} (derived from LEFEA with shell elements) and accounting for some influence of arching action in the one-way shear resistance for concentrated loads close to the support by β_{shear}:

$$V_{R,CSCT} = \frac{v_{R,shear} \cdot b_{eff}}{\beta_{shear}} \tag{4}$$

In this approach, the parameters that need to be evaluated in the numerical models are the distribution of unitary shear forces v (to calculate v_{avg} and b_{eff}), unitary bending moments m (to calculate m_{max}) and the total shear force going through the control section $V_{control}$ (Figure 5 – to calculate b_{eff}) for a given applied load. Alternatively, $V_{control}$ can be directly determined from beam statics. Further details on the numerical models will be given in the next sections.

The effective shear width b_{eff} is calculated by dividing the total shear force going through the evaluated direction along the slab width ($V_{control}$) by an averaged unitary shear force over the control sections v_{avg}[3,35] determined with the finite element model (Eq. (5)). To be consistent with the CSCT principles, the control section to calculate the averaged unitary shear forces and the maximum bending moments is placed at $0.5d_l$ from the edge of the support on cantilever slabs and at $0.5d_l$ from the face of the load for simply supported slabs (Figure 5a). The length of the control section (distribution width) over which v is averaged to calculate v_{avg} is assumed $4d_l$ for cantilever slabs and $4d_l + l_{load}$ for simply supported slabs (Figure 5). In other words, we use a distribution width to calculate an averaged shear force v_{avg} and the effective shear width b_{eff} is calculated based on v_{avg}:

$$b_{eff} = \frac{V_{control}}{v_{avg}} \tag{5}$$

The arching action that takes place for loads close to the support, which increases the one-way shear resistance for such conditions, is accounted for by β_{shear}[11] (Equation (6)). At this point, however, it shall be remembered that the CSCT was derived assuming flexural-shear failures and that the β_{shear} is only a simplification to allow estimating the enhanced resistance in the case of possible shear-compression failures.

$$\beta_{shear} = \frac{a_v}{2.75 \cdot d_l}, \text{ with } d_l \leq a_v \leq 2.75d_l \tag{6}$$

The shear and moment-related redistribution due to cracking is accounted for in the numerical models by assuming a Poisson ratio $\mu = 0$ and a reduced shear modulus ($G_c = E_c/16$)[3,36]. For slabs influenced by arching action (loads close to the support), using b_{eff} allows us to include the effect of the arching action in the load portion from F that is transferred directly to the support. Conversely, for slabs subjected to a load further away from the support, the use of b_{eff} could be suppressed. For such cases, someone could simply compare the design load F_{Ed} with the calculated load that causes a one-way shear failure $F_{predicted}$.
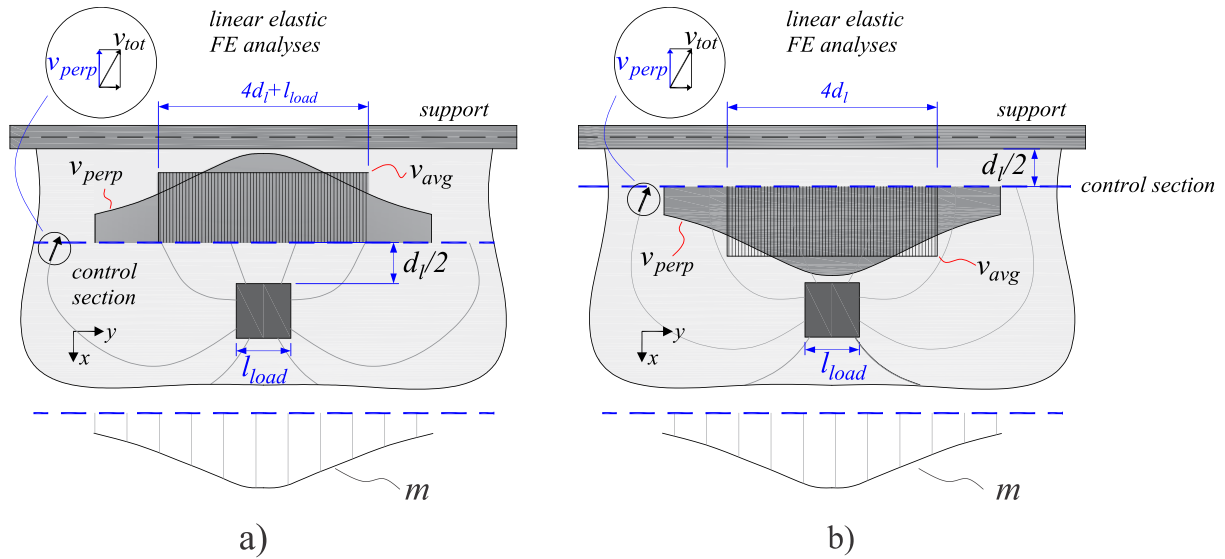
Figure 5 - Control section location and averaged shear force v_{avg} definition for a) simply supported slabs and b) cantilever slabs. Adapted from Natário[11].
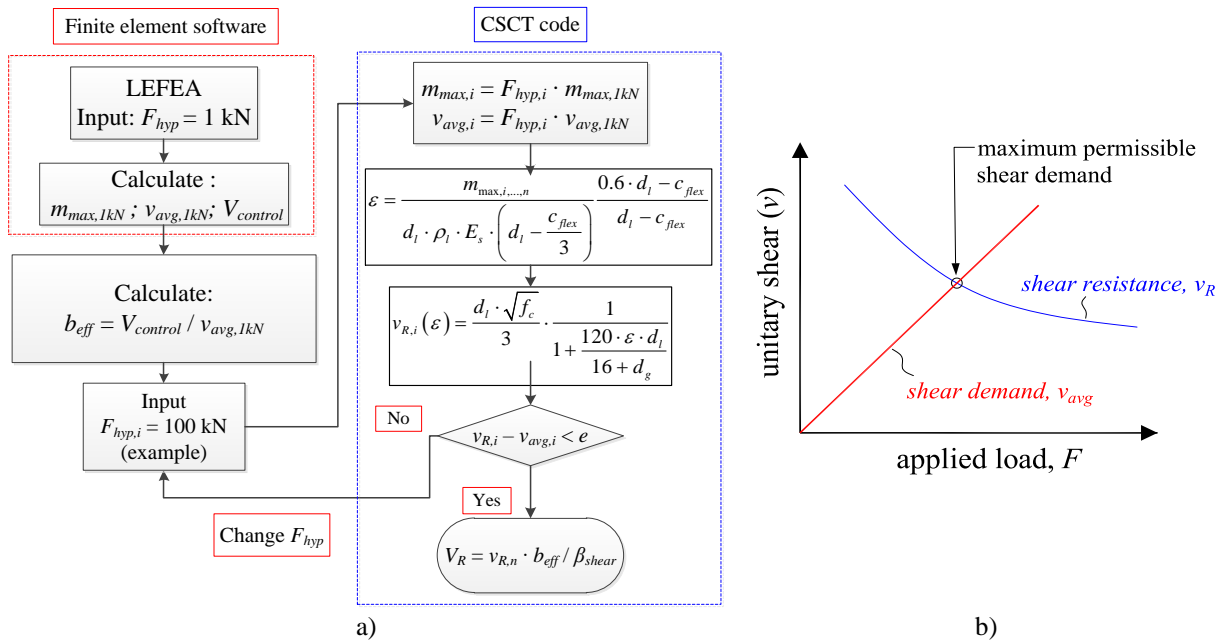

Figure 6 – a) Flowchart of the main steps for evaluating the one-way shear resistance following CSCT; b) Sketch of the iterative process combining the shear demand v_{avg} and shear resistance v_R. (SI units: 1 kN = 0.225 kip).

Figure 6a shows the flowchart of calculations performed combining LEFEA outputs with the CSCT shear expressions. Firstly, a unitary force $F_{hyp} = 1$ kN [0.225 kip] is applied to the numerical model to compute the averaged shear force $v_{avg,1kN}$ and the maximum bending moments $m_{max,1kN}$ over the control section. Then, the effective shear width b_{eff} is calculated according to Eq. (4) and Figure 5. In the end, a subroutine is used to find the applied concentrated load $F_{hyp,i}$ iteratively that equals the unitary shear resistance $v_{R,i}$ with the average shear demand $v_{avg,i}$ over the control section (see Figure 6b). When the iterative process ends, the one-way shear capacity (in force units) V_R is calculated, accounting for the effective shear width b_{eff} and the arching action for loads close to the support ($a_v < 2.75\ d_l$). With this procedure, the externally applied load ($F_{predicted}$) that causes the sectional shear failure and one-way shear resistance ($V_{R,CSCT}$) are predicted. $F_{predicted}$ is the last value of $F_{hyp,i}$ in the iterative process that makes $v_{R,i}$ is equal to $v_{avg,i}$.

Since the relation between the applied load and the sectional shear force depends only on the load position and support layout, the comparison between tested and predicted resistances could be performed directly in terms of the applied concentrated loads in the tests F_{test} and the predicted value $F_{predicted}$. In other words, for loads that are not influenced by arching action, the comparison between the tested and predicted failure loads ($F_{test}/F_{predicted}$) equals the ratio between tested and predicted shear resistances ($V_{test}/V_{predicted}$). Therefore, for such cases, the calculation of the effective shear width would not be necessary. In this study, however, the effective shear width was calculated for all tests as a way to include the influence of arching action when applicable, as recommended by Natário[11].

Refined approach for two-way shear analyses

The punching shear capacity is assessed by the CSCT ($\psi_x - \psi_y$) method[26,36] inspired by the work of Natário[11] with some small changes. In this method, the control perimeter is placed at $d_v/2$ from the load edges, where d_v is the mean depth of the flexural reinforcement in both directions. The CSCT expressions for punching shear assume that increasing the width of the critical shear crack w_{cr} reduces the strength of the compression strut carrying shear around the loaded area[29]. The width of the critical shear crack w_{cr} is assumed proportional to the product between the slab rotation ψ and the effective depth of the reinforcement d_v[25,29].

The CSCT considers the shear redistribution around the loaded area in a simplified way. In this method, the slab rotations depend on the considered direction and are uneven along the control perimeter, meaning that some parts of the slab reach their ultimate strength while others still have a potential strength capacity[11,26,36]. The control perimeter is usually divided into four segments assuming constant rotations ψ_x-ψ_y and unitary strengths $v_{R,x}$-$v_{R,y}$ for each segment. The control perimeter without round corners was adopted in the refined approach to simplify the post-processing of the numerical results. The punching shear strength is given by:

$$V_R = v_{R,x1} \cdot b_{0,x1} + v_{R,x2} \cdot b_{0,x2} + v_{R,y1} \cdot b_{0,y1} + v_{R,y2} \cdot b_{0,y2} \tag{7}$$

where $b_{0,ij}$ are defined in Figure 7 (i refer to the directions evaluated, direction x or y, and j refer to the side of the control perimeter in the evaluated direction, sides 1 or 2); the unitary/nominal shear strength in each segment $v_{R,ij}$ is calculated as[12] (SI units: f_c in MPa; d_g in mm; 1 MPa = 145 psi; 1 mm = 0.04 in.):

$$v_{R,ij} = \frac{(3/4) \cdot d_v \cdot \sqrt{f_c}}{1 + 15 \cdot \left[\psi_{ij} \cdot d_v / \left(d_g + d_{g0} \right) \right]} \tag{8}$$

$$d_{g0} = \begin{cases} 16, & \text{if } f_c < 70MPa \\ 0, & \text{if } f_c \geq 70MPa \end{cases} \tag{9}$$

The rotations ψ_{ij} in each side of the control perimeter were calculated according to Level of Approximation III from the *fib* Model Code provisions[12], which are based on the CSCT[25]. In each segment of the control perimeter, the rotation was calculated as:

$$\psi_{ij} = 1.2 \cdot \frac{r_{s,ij}}{d_i} \cdot \frac{f_{yi}}{E_s} \cdot \left(\frac{m_{s,ij}}{m_{R,i}} \right)^{3/2} \tag{10}$$

$$m_{s,ij} = \frac{1}{b_s} \cdot \int_{-b_s/2}^{+b_s/2} \left| m_{ij} \right| \cdot di \quad i \perp j$$

$$m_{s,x1} = \frac{1}{b_s} \cdot \int_{-b_s/2}^{+b_s/2} m_{x1} \cdot dy \; ; \; m_{s,x2} = \frac{1}{b_s} \cdot \int_{-b_s/2}^{+b_s/2} m_{x2} \cdot dy \; ; \; m_{s,y1} = \frac{1}{b_s} \cdot \int_{-b_s/2}^{+b_s/2} m_{y1} \cdot dx \; ; \; m_{s,y2} = \frac{1}{b_s} \cdot \int_{-b_s/2}^{+b_s/2} m_{y2} \cdot dx \tag{11}$$

Natário[11] explains that $r_{s,ij}$ is the distance between the center of the concentrated load and the point where the acting unitary bending moment in the direction of the relevant reinforcement is zero (Figure 7a), d_i is the effective flexural depth in the appropriate direction, f_{yi} is the steel yielding stress, E_s is Young's modulus of steel, $m_{s,ij}$ is the averaged acting bending moment at the loading plate edge ij within the width b_s (Figure 7c) and $m_{R,i}$ is the yielding moment per unit length in the evaluated direction. The support strip width b_s is calculated as:

$$b_s = \min \left\{ 1.5 \cdot \sqrt{r_{s,ij} \cdot r_{s,ji}} \right\} \quad i \perp j \tag{12}$$

$$b_{0,x1} = \frac{V_{x1}}{v_{x1,max}} \quad ; \quad b_{0,x1} = \frac{V_{x2}}{v_{x2,max}}$$

$$b_{0,y1} = \frac{V_{y1}}{v_{y1,max}} \quad ; \quad b_{0,y2} = \frac{V_{y2}}{v_{y2,max}}$$

$$b_s = \min \begin{bmatrix} 1.5 \cdot \sqrt{r_{s,x1} \cdot r_{s,y1}} \\ 1.5 \cdot \sqrt{r_{s,x1} \cdot r_{s,y2}} \\ 1.5 \cdot \sqrt{r_{s,x2} \cdot r_{s,y1}} \\ 1.5 \cdot \sqrt{r_{s,x2} \cdot r_{s,y2}} \end{bmatrix}$$
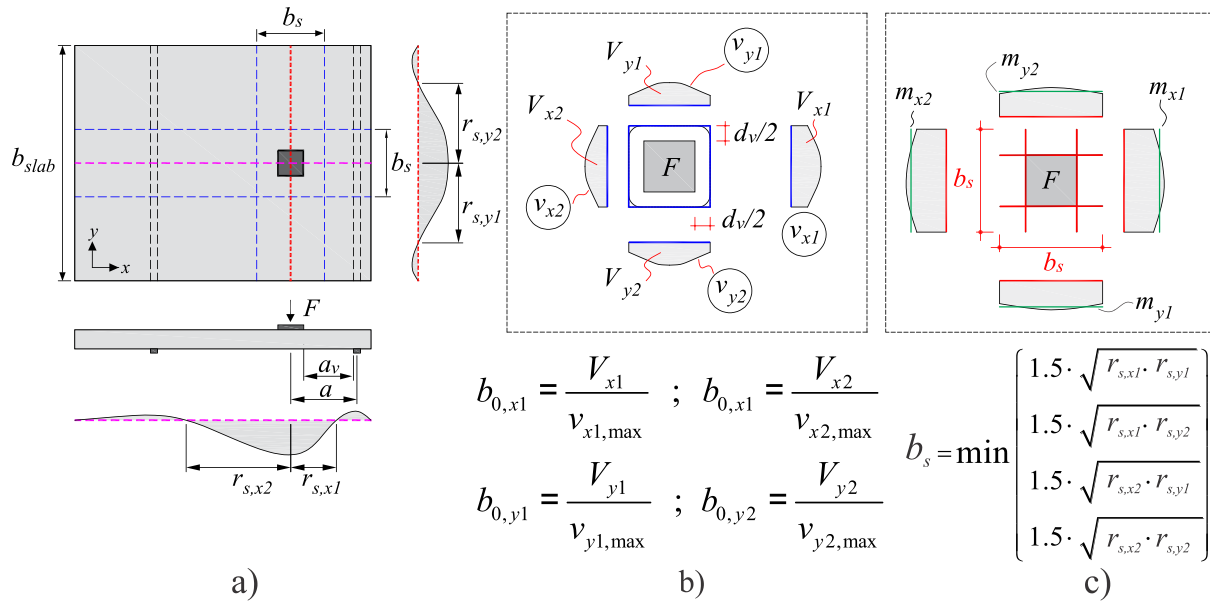
a)   b)   c)

Figure 7 - Definition of (a) r_{si} distances; b) reduced control perimeters for square loads; and c) averaged acting bending moments at the edges of the concentrated load and support strip widths. Adapted from Natário[11].

The length of each segment of the control perimeter ($b_{0,x1}$, $b_{0,x2}$, $b_{0,y1}$ and $b_{0,y2}$), calculated without rounded corners as in Natário[11], was given by the ratio between the maximum applied unitary shear force perpendicular to the control perimeter ($v_{x1,max}$, $v_{x2,max}$, $v_{y1,max}$ and $v_{y2,max}$,) and the total shear force going through that perimeter (V_{x1},V_{x2},V_{y1},V_{y2}) (Figure 7b).
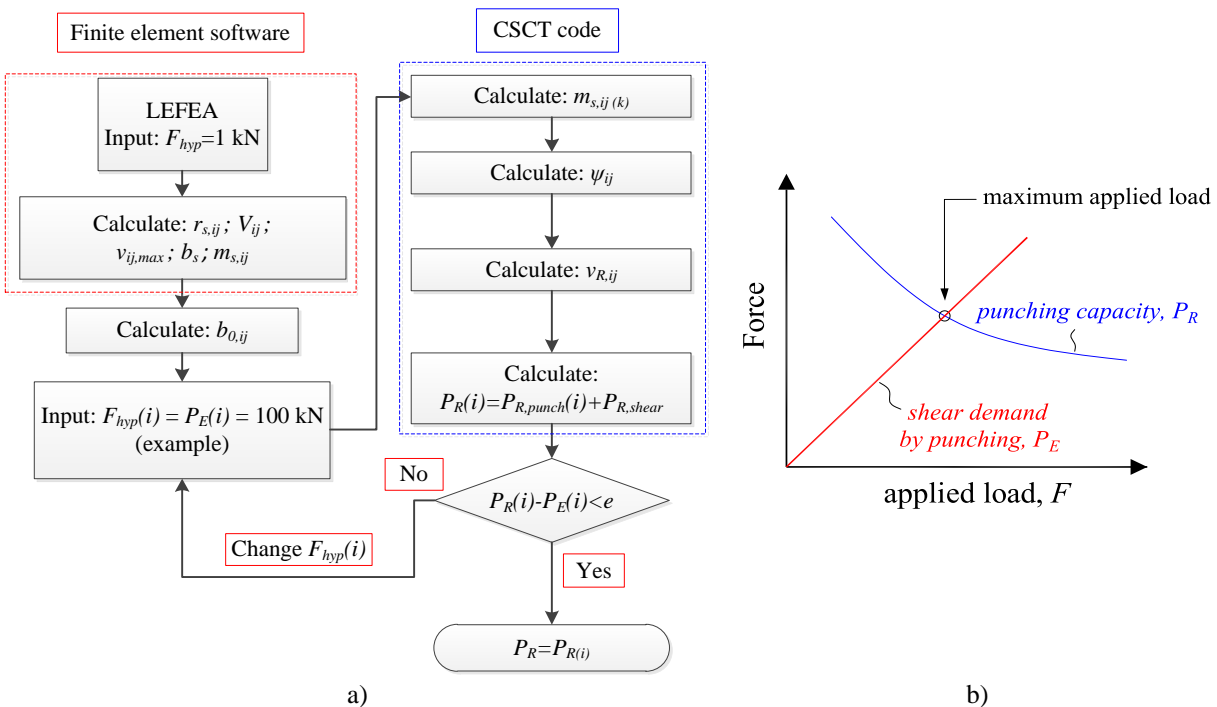

a)   b)

Figure 8 – a) Flowchart of the main steps for the evaluation of the punching capacity with the CSCT ($\psi_x - \psi_y$) method; b) Sketch of how the punching capacity is determined in the iterative process. (SI units: 1 kN = 0.225 kip).

Figure 8 shows the main steps to predict the punching shear capacity of slabs coupling LEFEA with the CSCT model

for non-axis-symmetrical punching[36]. First, a LEFEA is carried out to compute the distribution of shear forces ($v_{ij,max}$ = $v_{x1,max}$, $v_{x2,max}$, $v_{y1,max}$, $v_{y2,max}$) and averaged bending moments ($m_{s,ij}$ = m_{x1}, m_{x2}, m_{y1}, m_{y2}) over the control sections for an applied load equals 1 kN [0.225 kip]. At this step, the total shear force on each portion of the control perimeter (V_{x1}, V_{x2}, V_{y1} and V_{y2}) and the slab strip width b_s shall also be calculated. Afterwards, the reduced control perimeter segments $b_{0,ij}$ are calculated for each side of the control perimeter. These values are entered as input in a subroutine that calculates iteratively the punching load $P_E(i)$ that is equal to the punching resistance $P_R(i)$. Notably, the number of outputs of the LEFEA is higher than that required for one-way shear since control perimeter segments are applied.

A factor was derived by linear regression analyses to avoid overly unsafe predictions of punching capacity for the tests that failed as wide beams in shear (WB) highlighted in Figure 2b. Due to the shear flow characteristics of one-way slabs, a smaller portion of the load is transferred by the lateral sides of the control perimeter when the slab width is small (see Figure 9). As a consequence, these sides of the control perimeter may have a small contribution to the punching capacity for small values of b_{slab}/l_{load}. The influence of the ratio slab width-to-load size into the effective contribution of the sides of the control perimeter to the punching capacity (see Figure 9) was not considered by Natário[11] and is considered herein by multiplying the punching resistance $V_{R,y1}$ and $V_{R,y2}$ by a factor CF_{width}. This factor was derived assuming that the factor should vary between 0 and 1 and that the contribution of the lateral sides of the control perimeter increase by a square polynomial function. The constants of the polynomial function were adjusted to improve the predictions of punching capacity for a larger dataset of one-way slabs under concentrated loads presented by de Sousa et al.[9].
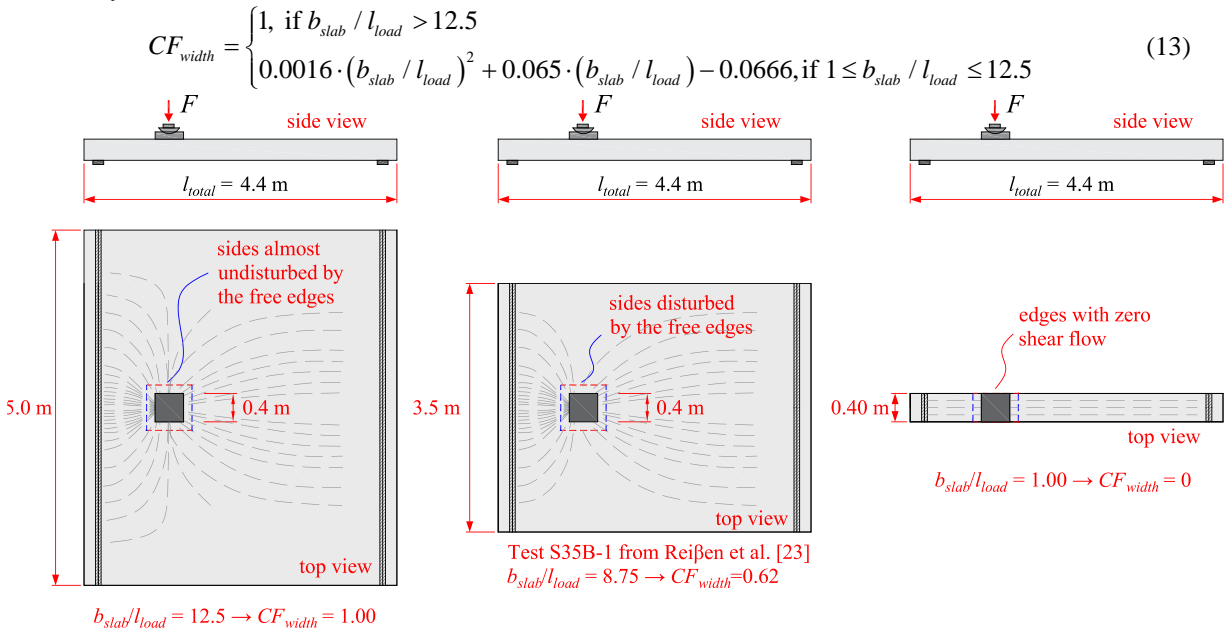
$$CF_{width} = \begin{cases} 1, \text{ if } b_{slab}/l_{load} > 12.5 \\ 0.0016 \cdot (b_{slab}/l_{load})^2 + 0.065 \cdot (b_{slab}/l_{load}) - 0.0666, \text{if } 1 \le b_{slab}/l_{load} \le 12.5 \end{cases} \tag{13}$$

Figure 9 - Influence of the ratio b_{slab}/l_{load} into the shear flow crossing the sides of the control perimeter parallel to the free edges. (SI units: 1 m = 3.3 ft).

Therefore, the following calculations are used to compute the contribution of each side of the control perimeter into the punching capacity (SI units: f_c in MPa; d_g in mm; 1 MPa = 145 psi; 1 mm = 0.04 in.):

$$V_{R,x1} = \frac{(3/4) \cdot d_v \cdot \sqrt{f_c}}{1 + 15 \cdot \left[\psi_{x1} \cdot d_v / (d_g + d_{g0}) \right]} \cdot b_{0,x1} \tag{14}$$

$$V_{R,x2} = \frac{(3/4) \cdot d_v \cdot \sqrt{f_c}}{1 + 15 \cdot \left[\psi_{x2} \cdot d_v / (d_g + d_{g0}) \right]} \cdot b_{0,x2} \tag{15}$$

$$V_{R,y1} = \frac{(3/4) \cdot d_v \cdot \sqrt{f_c}}{1 + 15 \cdot \left[\psi_{y1} \cdot d_v / (d_g + d_{g0}) \right]} \cdot b_{0,y1} \cdot CF_{width} \tag{16}$$

$$V_{R,y2} = \frac{(3/4) \cdot d_v \cdot \sqrt{f_c}}{1+15 \cdot \left[\psi_{y2} \cdot d_v / \left(d_g + d_{g0}\right)\right]} \cdot b_{0,y2} \cdot CF_{width} \tag{17}$$

The punching capacity for square loads or not elongated (rectangular) loads ($l_{load} < 3d_v$ and $b_{load} < 3d_v$) is then given by the sum of the capacities of the perimeter segments:

$$P_{R,punch} = V_{R,x1} + V_{R,x2} + V_{R,y1} + V_{R,y2} \tag{18}$$

Slabs subjected to elongated loads develop some particular characteristics that need to be considered. The shear flow assumes a radial pattern in the corners, with a high concentration of shear flow in these regions. Conversely, the shear flow in the elongated sides has lines almost parallel to each other with lower demand in this region (Figure 10a). Following the approach proposed by Natário[11] and inspired by the works from Sagaseta et al.[36], the contribution of the control perimeter in the corners is calculated by the two-way shear expressions ($P_{R,puch}$). In Natário's approach, the same expressions to calculate the one-way shear capacity of such slabs were used in the region with one-way shear behavior, which increased the post-processing effort of the numerical models. In this study, a simplification was performed on this part of the calculations based on the work from Setiawan et al.[37].
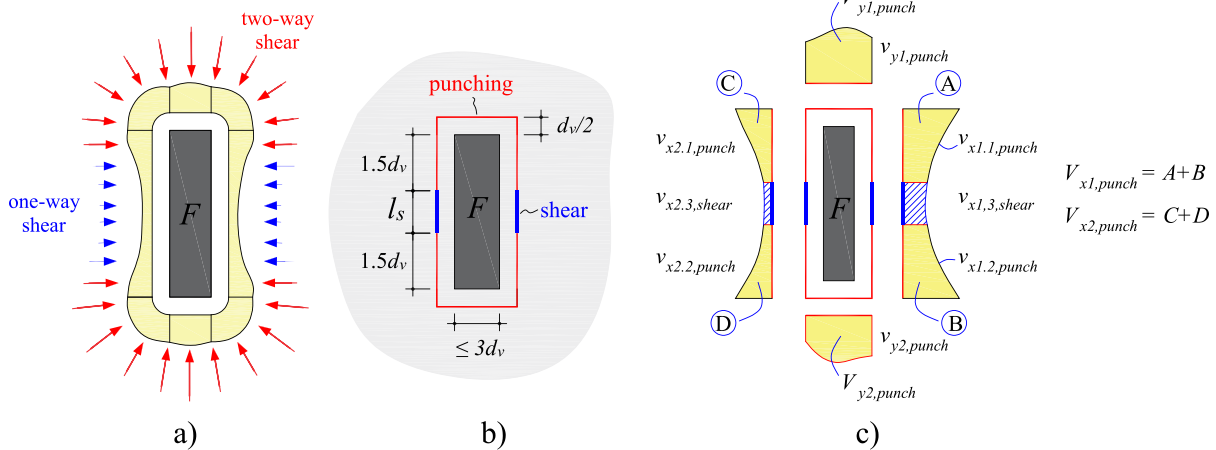

Figure 10 – a) Sketch of distribution of nominal shear forces along the control perimeter of elongated loads (assuming only two sides $> 3d_v$) with the concentration of shear forces at the corners; b) lengths of the sides of the control perimeter with two-way shear and one-way shear (control perimeter without rounded corners used in the calculations); c) sketch of the areas that shall be integrated to determine the shear force distribution around the control perimeter.

When the loaded area is elongated on one of the sides ($l_{load} > 3d_v$ or $b_{load} > 3d_v$), the contribution of the elongated sides not included in the computation of $b_{0,x1}$, $b_{0,x2}$, $b_{0,y1}$ and $b_{0,y2}$ shall be considered assuming a one-way shear behavior for such lengths (blue lines in Figure 10b). These limits to define the regions considered with two-way shear behavior or one-way shear behavior are based on the current *fib* Model Code 2010[12]. However, the control perimeter herein was defined without rounded corners to simplify the post-processing of the numerical models. In practice, four sides of the load can be higher than $3d_v$ and the shape of the load be square, but the idea remains similar to that applied for elongated loads.

In this study, the contribution of the sides l_s (Figure 10b) is computed according to Setiawan et al.[37] and Cavagnis et al.[38] (assuming only two sides of the load larger than $3d_v$):

$$P_{R,shear} = v_{c,min} \cdot (2 \cdot l_s) = \frac{k \cdot d_v \cdot \sqrt{f_c}}{\sqrt{\varepsilon_y \cdot \dfrac{d_v}{d_{dg}}}} \cdot (2 \cdot l_s) \tag{19}$$

Herein, $v_{c,min}$ is the minimum shear resistance per unit length (assuming reinforcement yielding), $k = 0.019$, $\varepsilon_y =$ is the flexural reinforcement yield strain ($= 0.0025$), l_s is the length of the sides assumed with one-way shear behavior (Figure 10), and d_{dg} is the parameter that considerers the crack roughness, which is calculated as follows (SI units: f_c in MPa; d_g in mm; 1 MPa = 145 psi; 1 mm = 0.04 in.):

$$d_{dg} = \min\left(40 \text{ mm}, 16 + d_g\right) \text{ for } f_c \leq 60 MPa$$

$$d_{dg} = \min\left(40 \text{ mm}, 16 + d_g \cdot \left(\frac{60}{f_c}\right)^2\right) \text{ for } f_c > 60 MPa \tag{20}$$

The total punching capacity for elongated loads is given by:

$$P_{predicted} = P_{R, punching} + P_{R, shear} \tag{21}$$

PROPOSED APPROACH FOR SIMPLIFIED CALCULATIONS

Proposed analytical approach for one-way shear predictions

The one-way shear resistance v_R was calculated with the same expressions described previously in the refined approach, assuming a beam behavior to determine the relation between F_{hyp}, m_i and v_i. In practice, this means using a static system of a beam with a unitary width to compute the unitary bending moments and shear forces assumed constant along this length. After defining the unitary shear resistance in the iterative process (Figure 6), the predicted sectional shear resistance is found multiplying the calculated unitary resistance by the predicted effective shear width.

As identified in previous studies[1,9], the French effective shear width ($b_{eff,french}$) works reasonably well when the governing failure mechanism is one-way shear. This occurs mainly when the load is placed at positions with a_v/d_l lower lower than 2.75 (the region that may benefit from arching action). Herein, a_v/d_l is the clear shear span to effective depth ratios. However, for thin slabs and slabs under a concentrated load far away from the support ($a_v/d_l > 2.75$), the predicted effective shear width with this approach may overestimate the one-way shear capacity[5,9]. This commonly occurs when the governing shear failure mode is punching instead of one-way shear. To solve this issue, this study proposes to use a modified effective shear width according to the clear shear span to depth ratio (a_v/d_l):

$$b_{eff, french} = l_{load} + 2 \cdot \left(b_{load} + a_v\right) \leq b_{slab}$$

$$CF_{shear} = -0.1143 \cdot a_v / d_l + 1.3143 \leq 1 \tag{22}$$

$$b_{eff, proposed} = b_{eff, french} \cdot CF_{shear} \begin{cases} \leq b_{slab} \\ \geq l_{load} + d_l \end{cases}$$

In this approach, the predicted effective shear width $b_{eff,proposed}$ decreases for large distances of the load to the support. Herein, it is assumed that when the shear transfer is not benefited from arching action ($a_v/d_l > 2.75$), the predicted effective shear width should be adjusted.
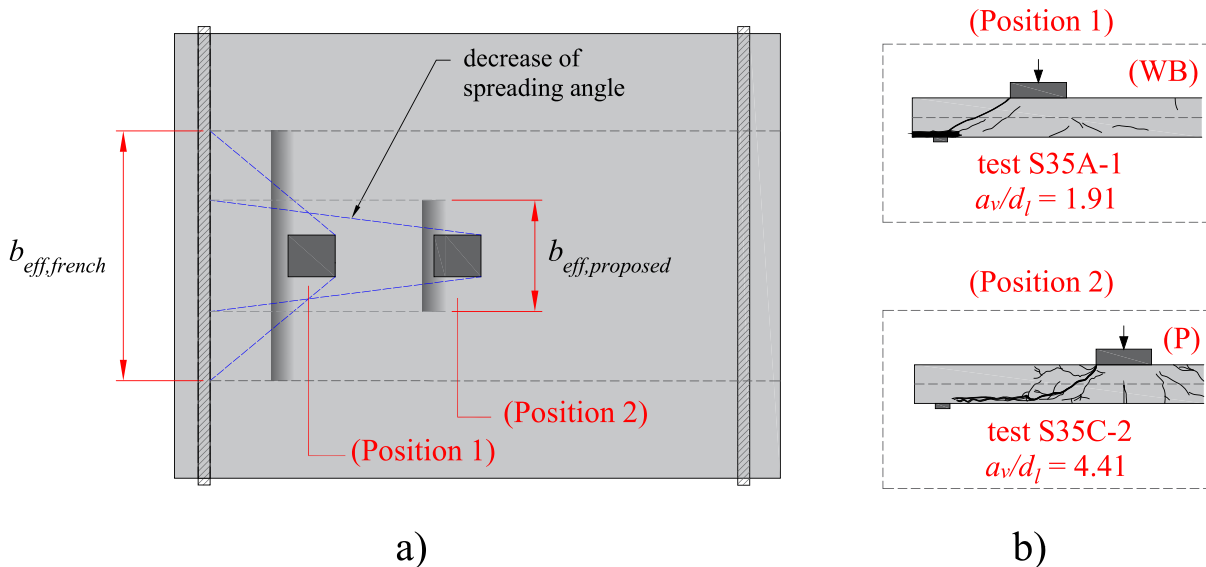

Figure 11 - Modified effective shear width according to the ratio a_v/d_l and b) cracking pattern of tests from Reißen et al.[23] varying the load position and that developed different failure shear mechanisms.

Figure 11a shows a sketch of the practical effect of CF_{shear} according to the load position. Moreover, Figure 11b shows the cracking pattern of tests performed by Reißen[8], which clearly indicates a change of governing failure mechanism by varying the load position and, hence, the clear shear span to effective depth ratio a_v/d_l.

Proposed analytical approach for two-way shear predictions

To allow a simplified estimation of the rotations without the use of LEFEA, we propose in this study to use expressions based on the ratio between the applied concentrated load P and the flexural resistance P_{flex} estimated by yield line analyses. The expressions used to compute the rotations around the loaded area of simply supported slabs are:

$$\psi_{x1} = 1.2 \cdot \frac{a}{d_l} \cdot \frac{f_{yl}}{E_s} \cdot \left(\frac{P}{P_{flex}} \right)^{3/2}$$

$$\psi_{x2} = 1.2 \cdot \frac{\left(l_{span} - a \right)}{d_l} \cdot \frac{f_{yl}}{E_s} \cdot \left(\frac{P}{P_{flex}} \right)^{3/2} \tag{23}$$

$$\psi_{y1} = \psi_{y2} = 1.2 \cdot \frac{\left(b_{slab} / 2 \right)}{d_t} \cdot \frac{f_{yt}}{E_s} \cdot \left(\frac{P}{P_{flex}} \right)^{3/2}$$

For a conservative prediction, the maximum rotation computed shall be used (ψ_{max}). In the proposed approach, the punching-resisting control perimeter is calculated without rounded corners (to allow a fair comparison with the approach based on LEFEA) and without any reduction due to the distribution of shear stresses on the perimeter (**Figure 7**b). Therefore, the sides of the control perimeter are calculated as:

$$b_{0,x1} = b_{0,x2} = \min\{l_{load}; 3 \cdot d_v\} + 1 \cdot d_v$$
$$b_{0,y1} = b_{0,y2} = \min\{b_{load}; 3 \cdot d_v\} + 1 \cdot d_v \tag{24}$$

Three yield line mechanisms, suggested by Belletti et al.[39], were evaluated to predict the flexural capacity of slabs under concentrated loads P_{flex} (**Figure 12**). A comparison between tested and predicted flexural capacities of slabs under concentrated loads using these yield lines was performed previously. Mechanism 1 (with the yield line extending across the whole slab width) provided the best fit with the experimental results. Therefore, the flexural capacity of the slabs was predicted by the following expression:
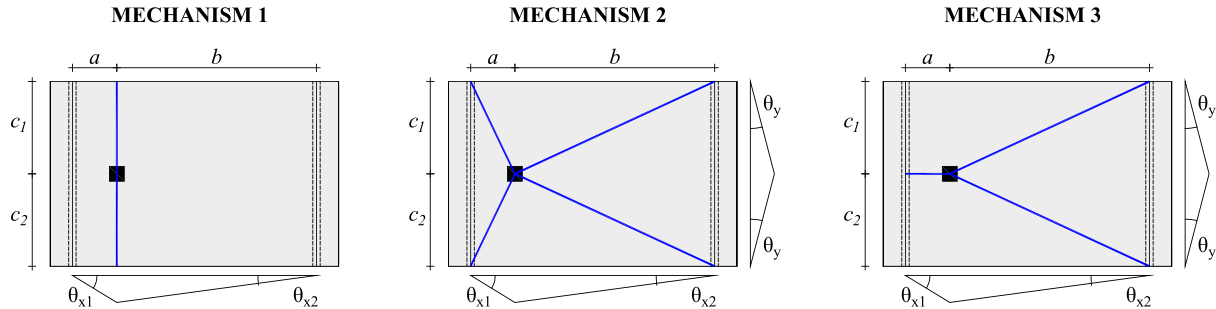
Figure 12 - Yield line mechanisms for simply supported slabs under CL based on Belletti et al.[39].

$$P_{flex} = \begin{cases} \dfrac{m_{R,x} \cdot b_{slab}}{a} + \dfrac{m_{R,x} \cdot b_{slab}}{(l_{span} - a)} - \left(l_{span} \cdot b_{slab} \cdot \gamma_{conc} \cdot h_{slab} \cdot 0.5 \right), & \text{for 1 load in the span} \\[2em] \dfrac{m_{R,x} \cdot b_{slab}}{a} - \left(l_{span} \cdot b_{slab} \cdot \gamma_{conc} \cdot h_{slab} \cdot 0.5 \right), & \text{for 2 symmetrical loads in the span} \end{cases} \tag{25}$$

The same factors and approaches used to compute the effect of the free edges on the contribution of the lateral sides of the control perimeter are applied in this simplified approach. The same calculations were also performed to compute the contribution of the elongated sides with predominant one-way shear when applicable.

PREDICTING THE GOVERNING SHEAR FAILURE MODE

In a design or assessment task, the most critical failure mechanism would be defined by the lower ratio between the design loads and load effects (V_{Rd}/V_{Ed} and P_{Rd}/P_{Ed}). Here, V_{Rd} and V_{Ed} are the design shear capacities and design shear actions, respectively. P_{Ed} and P_{Rd} are the respective design concentrated loads and design punching capacities. Knowing the tested concentrated loads and shear forces at failure (P_{test} and V_{test}) from the laboratory tests, Natário[11] suggests that the governing failure mode would be related to the maximum ratio between $P_{test}/P_{predicted}$ and $V_{test}/V_{predicted}$, where P_{test} and $P_{predicted}$ are the tested and predicted punching capacities, respectively; V_{test} and $V_{predicted}$ are tested and predicted one-way shear capacities. Since using the term one-way shear capacity for tests that failed by punching or punching capacity for the tests that failed by shear could be inconsistent, a different definition was used along with this study. The tested one-way shear capacity means the maximum sectional one-way shear occuring in the test. In the same way, the tested punching capacity means the externally applied load at failure. V_{test} and P_{test} include the influence of the self-weight. The tested one-way shear capacity considers the control section for computing the self-weight influence halfway between the load and the support.

Therefore, if the ratio $V_{test}/V_{predicted}$ is larger than $P_{test}/P_{predicted}$, one-way shear is theoretically more critical than punching shear, and the predicted governing failure mode is one-way shear. Another way to see how this makes sense is to look for the lower predicted resistance compared to the tested load (for shear and punching predictions), which also gives the larger ratio between tested and predicted resistances. In this study, the strength ratio SR = max $\{V_{test}/V_{predicted}; P_{test}/P_{predicted}\}$ is defined to predict the most critical failure mechanism without knowing the observed failure mode on the tests. Besides, this parameter is also used to investigate the level of conservatism of the investigated approaches combining the shear and punching predictions.

FINITE ELEMENT MODELS FOR THE REFINED APPROACH

In this study, the finite element software ABAQUS (version 6.14)[40] is used to evaluate the distribution of bending moments and shear forces at the control sections for one-way and two-way shear analyses (Figure 13). A 4-node shell element with reduced integration (S4R), hourglass control and finite membrane strains is used to simulate the slab. An 8-node linear brick element with reduced integration and hourglass control is used to simulate the plate supports (C3D8R). Interface properties of (i) hard contact (free to uplift) and (ii) frictionless are assumed at the contact between the plate supports and the slab surface. Alternatively, compression-only supports could be used along the support axis from the slab instead of including solid elements with interaction properties between the shell and solid elements, such as made by Natário[11]. The reinforcement was not modeled in the finite element models since its influence on the results was accounted for in the analytical shear and punching shear expressions.
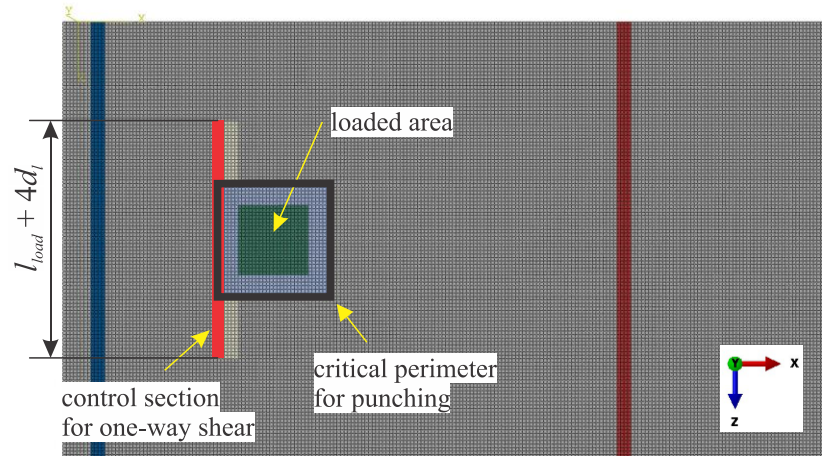
Figure 13 - Overview of the numerical models developed highlighting the evaluated regions for one-way shear and punching shear analyses.

The mesh size chosen varied according to the numerical models between 10 mm [0.39 in.] and 20 mm [0.78 in.]. In practice, the mesh size was chosen to assure a minimum amount of 8 elements distributed along the load edges. Based on mesh studies, the results seem to be mesh independent when at least 8 finite elements are distributed along the load edges. The vertical displacements are constrained at the support axis on the bottom face of the solid elements, simulating simple supports. The load is simulated by applying a uniform pressure with a resulting load equal to 1 kN

[0.225 kip] on the loading plate. Further details about the control sections and calculations of internal forces can be consulted elsewhere[4,11]. The concrete shear modulus used $G_{c,used}$ is taken as 1/8 of G_c based on Natário[11] with G_c:.

$$G_c = \frac{E_c}{2 \cdot (1 + \mu)} \tag{26}$$

The Poisson's coefficient μ is assumed as equal zero to account for the concrete cracking[3,11,18,36]. For simply supported slabs, a line of vertical displacement was constrained at the middle width of the support plates with free rotation (example in Figure 14).
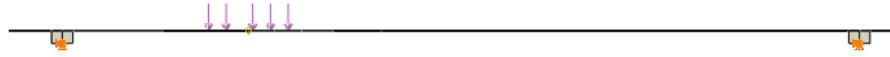

Figure 14 - Example of boundary conditions applied in the numerical models.

DATASET FROM LITERATURE

In this study, the same dataset used by Natário[11] (here named Dataset A) was investigated in order to allow a fair comparison between results. This dataset includes 48 tests from the following references: Damasceno[41], Ferreira[42], Regan and Rezai-Jarobi[43], and Reiβen et al.[23]. Only simply supported slabs were evaluated.

In this dataset, 30 tests were classified as failing by a clear punching (P, with none or some reinforcement yielding at failure). Two tests were classified as failing by a mixed-mode between one-way shear and two-way shear (WB+P) and 16 tests were classified as failing by one-way shear as wide beams (WB).

The majority of the tests were designed to achieve shear or punching failure modes. As a consequence, more than 95% of the tests have reinforcement ratios larger than 0.98%. All tests have a shear span to effective depth ratio a/d higher than 3. However, five tests were identified with ratio $a_v/d_l < 3$ and, hence, may have been influenced by the formation of direct compressive struts between the load and the support, such as identified in Figure 11b by the cracking pattern. The thickness of the tests varied between 100 mm [3.93 in] and 280 mm [11.02 in]. Due to the limited thickness in the tests with 100 mm [3.93 in] of thickness, some of these developed a punching failure with reinforcement yielding.

RESULTS

Predicting the most critical failure mode is one of the main tasks in the assessment of existing structures but is seldomly treated in the literature. Figure 15 compares the tested and predicted resistances for dataset A in terms of shear and punching capacities. The maximum strength ratio SR was calculated as the maximum of $V_{test}/V_{predicted}$ and $P_{test}/P_{predicted}$, and used to identify the most critical failure mechanism (theoretically). The most critical failure mechanism is the one providing the higher values between $V_{test}/V_{predicted}$ and $P_{test}/P_{predicted}$. Figure 15a,b,c uses only analytical expressions to define the effective shear width (one-way shear) and the punching capacity (using the ratio P/P_{flex} in calculating the slab rotations ψ). Figure 15d,e,f combines the outputs from LEFEA with the expressions based on the CSCT for shear and punching, such as proposed by Natário[11]. In this way, the benefits of using LEFEA can be investigated.

In Figure 15a, the average (AVG) ratio $V_{test}/V_{predicted}$ was 1.06, with a coefficient of variation (COV) equal to 15.4%. Using the punching expressions, the average ratio between tested and predicted resistances $P_{test}/P_{predicted}$ was 1.14 with a 13.1% of COV (Figure 15b). The lower scatter observed for the punching expressions is reasonable since most of the tests in the dataset developed a punching failure mode. In practice, the most unsafe predictions of one-way shear capacity occurred for the tests that failed by punching, and the most unsafe predictions of punching occurred for the tests that failed as wide beams in shear. In general, however, both approaches provided a good precision if considering the complexity of the problem.

Compared to the presented approach by Natário[11] (Figure 1), the results of the proposed analytical approach were slightly more accurate, which is expected since we calibrated the correction factors for shear and punching predictions to achieve a better performance of the proposed approach. Besides, the predictions of the punching capacity using the proposed analytical recommendations were more precise and conservative because the influence of the slab width and load size was considered by CF_{width} (see Figure 2b). The ratio SR achieved an AVG equal to 1.18 with a COV equal to 12.6% (Figure 15c), which is a level of accuracy and precision comparable to the models of one-way shear or two-

way shear expressions used to evaluate datasets of beams[28] and flat slabs[25]. The correct failure mechanism was determined in 69% of the tests, which is also interesting since only analytical expressions were used.

Similar results were observed combining the outputs from LEFEA into the CSCT expressions (Figure 15d,e,f). First, the one-way shear expressions provided an AVG ratio equal to 1.16 with a COV equal to 13.3% (Figure 15d). Therefore, the level of precision of the one-way shear expressions was excellent, even though most tests in Dataset A failed by punching. This occurs because the most critical section for one-way shear and punching are close to the load edge and, when the one-way shear resistance at the face of the load is achieved, the punching capacity of the slab will also be critical in this region. Proof of this explanation is that an asymmetrical punching cone, with the critical shear crack visible at only the face of the load, was identified in the tests of Reiβen et al.[23] that failed by punching (Figure 11b). Herein, it should be noted that the factor CF_{shear} was not applied in the approach including LEFEA for one-way shear predictions.

a) V_{test}/V_{pred} using analytical expressions ($b_{eff,proposed}$ as suggested in equation (23))

b) P_{test}/P_{pred} using analytical expressions (YLM for ψ)

c) SR based on a) and b) results

d) V_{test}/V_{pred} combining LEFEA with the CSCT expressions for shear[28]

e) P_{test}/P_{pred} combining LEFEA with the CSCT expressions for punching[25]
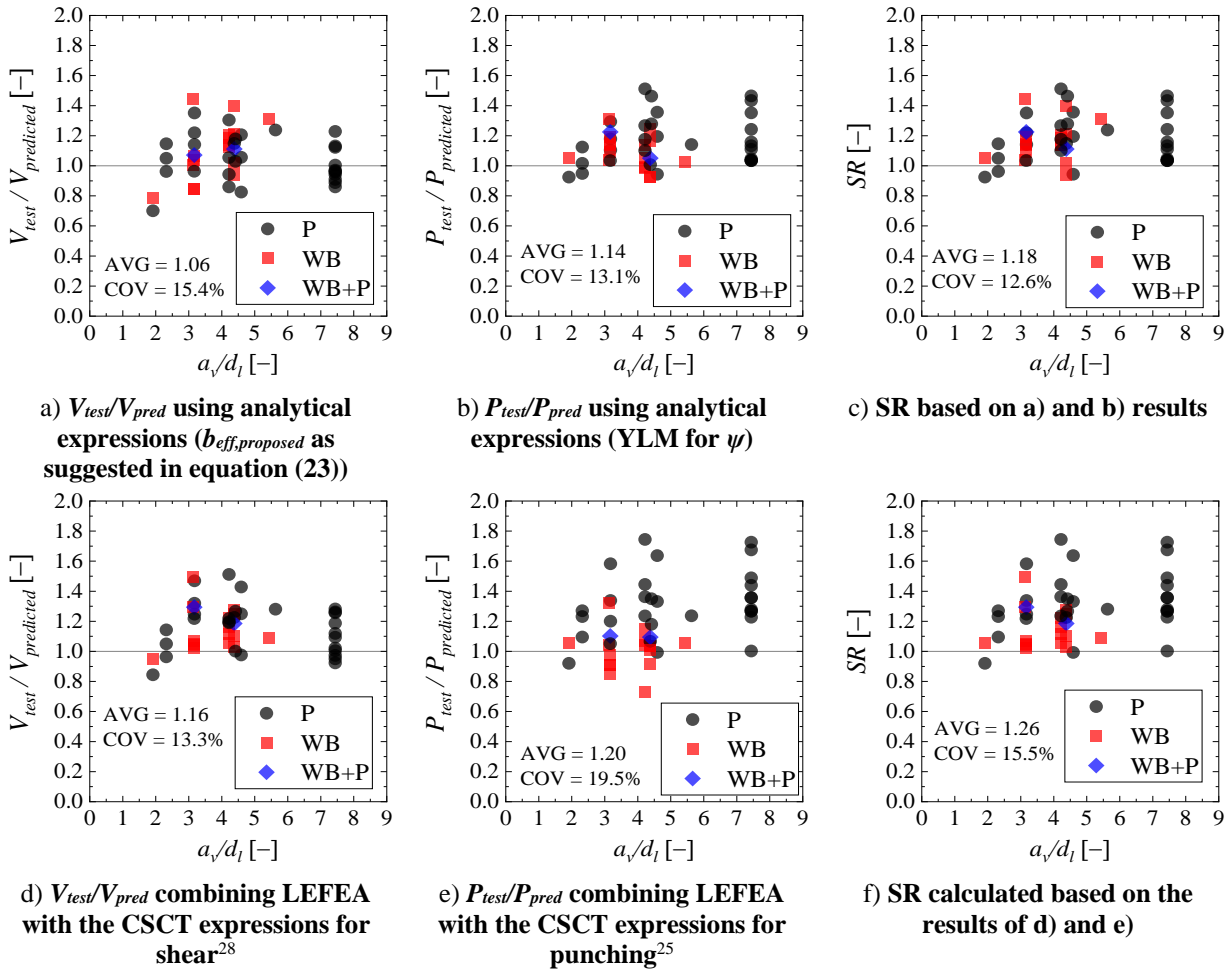
f) SR calculated based on the results of d) and e)

Figure 15 - Comparison between tested and predicted resistances for shear and punching and statistics of tested to predicted values. Notes: P = punching; WB = wide beam shear failure (one-way shear); WB+P = mixed failure mode or not clear between WB and P.

The punching expression combined with LEFEA reached an average ratio equal to 1.18 with a coefficient of variation of 19.5% (Figure 15e). Therefore, the predictions in the proposed approach using LEFEA were slightly better than those presented by Natário[11] (see Figure 2b). In practice, the predictions of punching capacity improved for the tests that failed as wide beams in shear using LEFEA and including the semi-empirical factor CF_{width} related to the ratio b_{slab}/l_{load}. The average strength ratio SR was 1.26 with COV equal to 14.7% (Figure 15e). The correct failure mechanism was predicted in 88% of the cases. Therefore, using LEFEA allowed improving the predictions of the governing failure mechanism and decreasing the conservatism of the predictions slightly. Comparatively, Natário[11]

correctly predicted the governing failure mechanism in 69% of the cases (Figure 2) using a similar approach and including LEFEA.

DISCUSSIONS

Most studies related to one-way slabs under concentrated loads close to the support focused on the assessment by the combination of one-way shear models with an effective shear width[3,5,17,23]. Besides, most models of effective shear width[9,44] based on the horizontal spreading of the load to the support predict an increasing effective shear width by increasing the clear shear span a_v or the ratio a_v/d_l. Based on this, a larger shear capacity $V_{predicted}$ could be expected for slabs under loads at large distances from the support if the shear slenderness effect is not accounted for in the one-way shear resistance expressions, such as and ACI 318-19[45], for instance. If the shear slenderness is accounted for, as for the CSCT expressions[25,28] which include the influence of the bending moment, an increase of the effective shear width could be counterbalanced by the decrease of the unitary shear resistance by increasing a_v/d_l. Consequently, the sectional shear at failure V_{test} would not be as much influenced by a_v/d_l.

For larger ratios a_v/d_l (for instance, > 4), slabs commonly fail by punching or in a transitional failure mode between one-way shear and two-way shear[4,15] or in flexure. Because of this, the available one-way shear capacity may eventually not be reached. In this case, the predictions of one-way shear capacity using only analytical expressions may become unsafe, such as observed in other publications[2,5] when using the French effective shear width. In this study, this problem was countered in the fully analytical approach by including a semi-empirical factor to decrease the effective shear width predicted with the French approach when the shear slenderness increases. In the approach using LEFEA, the predicted effective shear width (Figure 6) provides a conservative measurement even for the tests that failed by punching (Figure 15a). When evaluating the punching capacity of one-way slabs, conversely, the effect of the slab width and load size play a marked influence on the predictions. Lantsoght et al.[2] and Natário[11] found unsafe predictions of punching capacity for many tests that failed as wide beams using different approaches (fully analytical or combined with LEFEA). Until now, no specific publication addressed this problem, which was simplistically accounted for in this study by a semi-empirical factor CF_{width} that considers a lower contribution for some edges of the control perimeter depending on the relation between the slab width and the load size in the width direction.

In this study, we used a comparison between the ratios $V_{test}/V_{predicted}$ and $P_{test}/P_{predicted}$ to determine the most critical failure mechanism. In practice, one could also perform a comparison between the predicted load F that causes a one-way shear failure and F that causes a punching failure to determine the most critical value of the concentrated load. However, in this study, this approach was not used because it would require further adjustments on how to include the effect of arching action on the predicted failure load F.

One of the main ideas of using Levels of Approximations is that improved predictions of shear and punching capacity could be achieved by devoting more time and computational effort to estimating parameters required in the expressions[12]. In this study, the statistical properties of the analytical approach were slightly more accurate than the refined one due to the way in which the correction factors were derived in the fully analytical approach. The predictions using the simpler approach (only analytical expressions) can become more conservative, as would be expected in a Level of Approximation I, by multiplying the factors CF_{width} and CF_{shear} by reduction factors not included herein. It draws our attention that both simplified and refined approaches led to a small coefficient of variation in the predictions (COV $< 20\%$). In addition to allowing a broad insight into the distribution of shear and internal moments of the slabs, the data from LEFEA allowed improving predicting the governing failure mechanism, which increased from 69% at LoA I to 88% at LoA II. In practice, it can be stated that the refined approach is a more powerful tool since it may be extended directly to most complex cases not covered in laboratory tests.

CONCLUSIONS

In this study, the one-way and two-way shear expressions based on the CSCT were investigated from different viewpoints: (i) how accurate these expressions can be to predict the most critical shear failure mode of slabs that failed in different modes using only analytical expressions or combined to LEFEA and (ii) how the predictions are improved using LEFEA to predict the correct failure mechanism. From this study, the following conclusions can be drawn:

- The proposed approach using only analytical expressions combined with the CSCT allows predicting precisely the shear and punching capacity of simply supported slabs in a conservative way, regardless of the governing failure mechanism of the tests. The predictions of the shear and punching capacity were improved

by including two semi-empirical factors related to the transition from one-way shear to punching failures according to parameters such as the ratio a_v/d_l or b_{slab}/l_{load}.

- The coupling of the CSCT expressions with LEFEA allows improving the predictions of the governing failure mechanism. In practice, this approach is more suitable for the assessment of existing structures when higher levels of approximation are required.

- The transition of the governing failure mechanisms according to parameters such as the shear slenderness and the slab width to load size can be reasonably captured with the proposed semi-empirical factors.

- One of the main advantages of using LEFEA to assess the shear and punching capacity of slabs under concentrated loads is that a more precise prediction of the governing failure mechanism is achieved. Besides that, the distribution of shear forces and moments around the interest according to the boundary conditions are captured more realistically.

In summary, LEFEA is an interesting tool for assessing existing structures or reaching a more rational design of new structures since it allows to predict more accurately the governing failure mechanism of slabs. At the same time, the proposed analytical expressions have been shown to lead to good results for the shear and punching capacity in the absence of finite element software.

ACKNOWLEDGEMENTS

LIST OF NOTATIONS

a	= shear span: distance between the center of the support and the center of the load
a_v	= clear shear span: distance between face of support and face of load
b_0	= length of the critical perimeter
$b_{0,red}$	= reduced control perimeter
$b_{0,ij}$	= side of the control perimeter
b_{eff}	= effective shear width
$b_{eff,prop.}$	= proposed effective shear width
$b_{eff,french}$	= French effective shear width
b_{slab}	= slab width
b_{load}	= size of the concentrated load in the slab width direction
b_s	= strip width used to calculate m for punching capacity analyses
c_{flex}	= height of the compression zone
d_v	= average effective depth of reinforcement
d_l	= effective depth towards longitudinal steel
d_t	= effective depth towards transverse steel
d_g	= maximum aggregate size
d_{g0}	= reference aggregate size (= 16 mm)
d_{dg}	= parameter that considerers the crack roughness
f_c	= average compressive strength
f_{yi}	= steel yielding stress in the evaluated direction
h_{slab}	= slab thickness
k	= constant for one-way shear strength analyses in [38]
l_{span}	= span length
l_{load}	= size of the concentrated load in the span direction

l_s = is the length of the sides with one-way shear behavior

$m_{R,I}$ = yielding moment per unit length in the evaluated direction

m_{max} = maximum bending moment at the control section for a given applied load

$m_{s,ij}$ = averaged acting bending moment at the loading plate edge ij within the width b_s

$r_{s,ij}$ = distance between the center of the concentrated load and the point of contraflexure

v = shear force per unit length (nominal shear force)

$v_{c,min}$ = minimum shear resistance per unit length in [37]

v_{perp} = unitary shear force (shear force per unit length)

$v_{perp,max}$ = maximum nominal shear force (shear force per unit length)

v_{avg} = averaged shear force (shear force per unit length)

$v_{R,shear}$ = unitary one-way shear resistance

w_{cr} = width of the critical shear crack

E_c = modulus of elasticity of concrete

E_s = steel modulus of elasticity

CF_{width} = correction factor that considers the ratio b_{slab}/l_{load}

CF_{shear} = correction factor for the effective shear width

F = applied concentrated load

F_{Ed} = design concentrated load

$F_{predicted}$ = predicted load that causes a one-way shear failure or two-way shear failure

F_{hyp} = arbitrary concentrated load

G_c = shear modulus

$V_{control}$ = total shear force going through the evaluated direction along the slab width

V_{test} = maximum sectional shear achieved in the tests

$V_{predicted}$ = predicted shear resistance

V_{Rd} = design shear capacities

$V_{R,CSCT}$ = predicted one-way shear resistance with the CSCT expressions

$V_{R,ij}$ = punching shear strength corresponding to $b_{0,ij}$

V_{Ed} = design shear actions

P_{test} = maximum applied concentrated load at failure

P_{Ed} = design concentrated loads

P_{Rd} = design punching capacities

$P_{predicted}$ = predicted punching resistance

P_{flex} = concentrated load associated with the slab flexural capacity

$P_{R,shear}$ = total shear force resisted by one-way shear mechanisms for punching resistance analyses

$P_{R,punc}$ = total shear force resisted by punching shear mechanisms

β_{shear} = enhancement factor to account for arching action

ρ_l and ρ_t = flexural reinforcement ratios in longitudinal and transversal directions

ψ = rotations around the loaded area

ψ_{ij} = rotations in each side of the control perimeter

ε = strain in the control depth for one-way shear analyses

ε_y = is the flexural reinforcement yield strain

γ = concrete specific weight (assumed = 24 kN/m³ in this study)

μ = Poisson's coefficient

AVG = average

COV = coefficient of variation

P = observed failure mode is punching failure

WB = observed failure mode is wide beam shear failure

WB+P = the observed failure mode combines characteristics of WB and P

REFERENCES

1. Lantsoght, E. O. L., van der Veen, C., and Walraven, J. C. "Shear in one-way slabs under concentrated load close to support," *ACI Structural Journal*, V. 110, No. 2, 2013, pp. 275–84.

2. Lantsoght, E. O. L., van der Veen, C., Walraven, J. C., et al. "Database of wide concrete members failing in shear," *Magazine of Concrete Research*, V. 67, No. 1, 2015, pp. 33–52.

3. Natário, F., Fernández Ruiz, M., and Muttoni, A. "Shear strength of RC slabs under concentrated loads near clamped linear supports," *Engineering Structures*, V. 76, No. September, 2014, pp. 10–23.

4. de Sousa, A. M. D., Lantsoght, E. O. L., Setiawan, A., et al. "Transition from one-way to two-way shear by coupling LEFEA and the CSCT models." Proceedings of the fib Symposium 2021, Concrete Structures: New Trends for Eco-Efficiency and Performance. Lisbon, Portugal, 2021.

5. Halvonik, J., Vidaković, A., and Vida, R. "Shear Capacity of Clamped Deck Slabs Subjected to a Concentrated Load," *Journal of Bridge Engineering*, V. 25, No. 7, 2020, p. 04020037.

6. FD P 18-717. "Eurocode 2 - Calcul des structures en béton - Guide d'application des normes NF EN 1992," 2013.

7. Bui, T. T., Abouri, S., Limam, A., et al. "Experimental investigation of shear strength of full-scale concrete slabs subjected to concentrated loads in nuclear buildings," *Engineering Structures*, V. 131, 2017, pp. 405–20.

8. Reißen, K. "Zum Querkrafttragverhalten von einachsig gespannten Stahlbe- tonplatten ohne Querkraftbewehrung unter Einzellasten." Doctor of Engineering, PhD Thesis (Doctor of Engineering), Faculty of Civil Engineering, RWTH Aachen University, Aachen, Germany, 2016.

9. de Sousa, A. M. D., Lantsoght, E. O. L., Yang, Y., et al. "Extended CSDT model for shear capacity assessments of bridge deck slabs," *Engineering Structures*, V. 234, 2021, p. 111897.

10. Sousa, A. M. D., and el Debs, M. K. "Shear strength analysis of slabs without transverse reinforcement under concentrated loads according to ABNT NBR 6118:2014," *IBRACON Structures and Materials Journal*, V. 12, No. 3, 2019, pp. 658–93.

11. Natário, F. "Static and Fatigue Shear Strength of Reinforced Concrete Slabs Under Concentrated Loads Near Linear Support." PhD Thesis (Docteur ès Sciences), École Polytechnique Fédérale de Lausanne, 2015.

12. Fédération Internationale du Béton (fib). "fib Model Code for Concrete Structures 2010," v. vol. 1–2, Lausanne, Switzerland, Ernst & Sohn - fédération internationale du béton, Bulletin 65, 2012.

13. Rombach, G., and Henze, L. "Querkrafttragfähigkeit von Stahlbetonplatten ohne Querkraftbewehrung unter konzentrierten Einzellasten," *Beton- und Stahlbetonbau*, V. 112, No. 9, 2017, pp. 568–78.

14. Vida, R., and Halvonik, J. "Experimentálne overovanie šmykovej odolnosti mostovkových dosiek (Experimental verification of shear resistance of bridge deck slabs)," *Inžinierske stavby/Inženýrské stavby*, No. 4, 2018, pp. 2–6.

15. Lantsoght, E. O. L., van der Veen, C., Walraven, J. C., et al. "Transition from one-way to two-way shear in slabs under concentrated loads," *Magazine of Concrete Research*, V. 67, No. 17, 2015, pp. 909–22.

16. Fernández Ruiz, M., Vaz Rodrigues, R., and Muttoni, A. "Dimensionnement et vérification des dalles de roulement des ponts routiers," Rapport: Projet de recherche AGB 2002/028 sur demande du Groupe de travail Recherche en matière de ponts (AGB), 2009.

17. Henze, L., Rombach, G. A., and Harter, M. "New approach for shear design of reinforced concrete slabs under concentrated loads based on tests and statistical analysis," *Engineering Structures*, V. 219, No. May, 2020, p. 110795.

18. Vaz Rodrigues, R., Fernández Ruiz, M., and Muttoni, A. "Shear strength of R/C bridge cantilever slabs," *Engineering Structures*, V. 30, 2008, pp. 3024–33.

19. Goldbeck, A. T. "The Influence of Total Width of the Effective Width of Reinforced-Concrete Slabs Subjected to Central Concentrated Loading," *ACI Journal Proceedings*, V. 13, No. 2, 1917, pp. 78–88.

20. Lantsoght, E. O. L., de Boer, A., and van der Veen, C. "Distribution of peak shear stress in finite element models of reinforced concrete slabs," *Engineering Structures*, V. 148, 2017, pp. 571–83.

21. Goldbeck, A. T., and Smith, E. B. "Tests of Large Reinforced Concrete Slabs," *ACI Journal Proceedings*, V. 12, No. 2, 1916, pp. 324–33.
22. Lantsoght, E. O. L., van der Veen, C., de Boer, A., et al. "Influence of width on shear capacity of reinforced concrete members," *ACI Structural Journal*, V. 111, No. 6, 2014, pp. 1441–9.
23. Reißen, K., Classen, M., and Hegger, J. "Shear in reinforced concrete slabs-Experimental investigations in the effective shear width of one-way slabs under concentrated loads and with different degrees of rotational restraint," *Structural Concrete*, V. 19, No. 1, 2018, pp. 36–48.
24. Lantsoght, E. O. L., van der Veen, C., Walraven, J. C., et al. "Peak shear stress distribution in finite element models of concrete slabs." In: Zingoni, A., ed. Research and Applications in Structural Engineering, Mechanics and Computation. London, UK, CRC Press, Taylor & Francis Group, 2013. pp. 475–80.
25. Muttoni, A. "Punching Shear Strength of Reinforced Concrete Slabs without Transverse Reinforcement," *ACI Structural Journal*, V. 105, No. 4, 2008, pp. 440–50.
26. Sagaseta, J., Muttoni, A., Fernández Ruiz, M., et al. "Non-axis-symmetrical punching shear around internal columns of RC slabs without transverse reinforcement," *Magazine of Concrete Research*, V. 63, No. 6, 2011, pp. 441–57.
27. Muttoni, A., and Fernandez Ruiz, M. "Shear in slabs and beams: should they be treated in the same way?" FIB Bulletin 57: shear and punching shear in RC and FRC elements. 2010. pp. 105–28.
28. Muttoni, A., and Fernandez Ruiz, M. "Shear Strength of Members without Transverse Reinforcement as Function of Critical Shear Crack Width," *ACI Structural Journal*, V. 105, No. 2, 2008, pp. 163–72.
29. Muttoni, A., and Schwartz, J. "Behavior of Beams and Punching in Slabs without Shear Reinforcement," *IABSE Colloquium*, V. 62, No. January 1991, 1991, pp. 703–8.
30. Kani, G. N. J. "The Riddle of Shear Failure and its Solution," *ACI Journal Proceedings*, V. 61, No. 4, 1964, pp. 441–68.
31. Walraven, J. C. "Fundamental Analysis of Aggregate Interlock," *Journal of the Structural Division, ASCE*, V. 107, No. 11, 1981, pp. 2245–2270.
32. Dulacska, H. "Dowel Action of Reinforcement Crossing Cracks in Concrete," *ACI Journal Proceedings*, V. 69, No. 12, 1972, pp. 754–7.
33. Taylor, H. P. "Investigation of the dowel shear forces carried by the tensile steel in reinforced concrete beams," *Cement and Concrete Association*, 1969.
34. Vecchio, F. J., and Collins, M. P. "The Modified Compression-Field Theory for Reinforced Concrete Elements Subjected to Shear," *ACI Journal Proceedings*, V. 83, No. 2, 1986, pp. 219–31.
35. Belletti, B., Scolari, M., Muttoni, A., et al. "Shear strength evaluation of RC bridge deck slabs according to CSCT with multi – layered shell elements and PARC_CL Crack Model." IABSE Conference Geneva 2015. Geneva, Switzerland, 2015. pp. 1158–65.
36. Sagaseta, J., Tassinari, L., Fernández Ruiz, M., et al. "Punching of flat slabs supported on rectangular columns," *Engineering Structures*, V. 77, 2014, pp. 17–33.
37. Setiawan, A., Vollum, R. L., Macorini, L., et al. "Punching of RC slabs without transverse reinforcement supported on elongated columns," *Structures*, V. 27, 2020, pp. 2048–68.
38. Cavagnis, F., Fernández Ruiz, M., and Muttoni, A. "A mechanical model for failures in shear of members without transverse reinforcement based on development of a critical shear crack," *Engineering Structures*, V. 157, 2018, pp. 300–15.
39. Belletti, B., Damoni, C., Hendriks, M. A. N., et al. "Analytical and numerical evaluation of the design shear resistance of reinforced concrete slabs," *Structural Concrete*, V. 15, No. 3, 2014, pp. 317–30.
40. Dassault Systems Simulia Corp. "Abaqus Analysis user's manual 6.14," Providence, Rhode Island (USA), Dassault Systems Simulia Corp., 2014.
41. Damasceno, L. S. R. "Experimental analysis of one-way reinforced concrete flat slabs in punching shear with rectangular columns (in Portuguese: Análise experimental de lajes lisas unidirecionais de concreto armado com pilares retangulares ao puncionamento)." Masters' thesis, Departamento de Engenharia Civil, Universidade Federal do Pará, 2007.
42. Ferreira, M. de P. "Experimental analysis of one-way reinforced concrete flat slabs in axis or non-axis-symmetric punching shear (in Portuguese: Análise experimental de lajes lisas unidirecionais de concreto armado ao puncionamento simétrico ou assimétrico)." Masters' thesis, Universidade Federal do Pará, 2006.
43. Regan, P. E., and Rezai-Jorabi, H. "Shear Resistance of One-Way Slabs Under Concentrated Loads.," *ACI Structural Journal*, V. 85, No. 2, 1988, pp. 150–7.
44. Lantsoght, E. O. L., de Boer, A., van der Veen, C., et al. "Effective shear width of concrete slab bridges," *Proceedings of the Institution of Civil Engineers - Bridge Engineering*, V. 168, No. 4, 2015, pp. 287–98.

45.   ACI Committee 318. "Building Code Requirements for Structural Concrete (ACI 318-19)," 2019, p. 988.